# Identification of the parameters of an image-based model using integrated Digital Volume Correlation

L. Turpin[1,2,3], J. Bénézech[2,3], S. Roux[1]

lturpin@ens-paris-saclay.fr

1: Laboratoire de Mécanique Paris-Saclay (LMPS), Gif-sur-Yvette, France

2: Laboratoire des Composites Thermo-Structuraux (LCTS), Pessac, France

3: Safran Ceramics, Mérignac, France

# Ceramic Matrix Composites for aircraft engines

- 3D-woven SiC/SiC CMCs
  - high stiffness
  - stable mechanical properties wrt temperature

  → Hot parts
    - increase operating temperature
    - 1300°C → 1500°C
    - increase efficiency
  - complex mesostructure

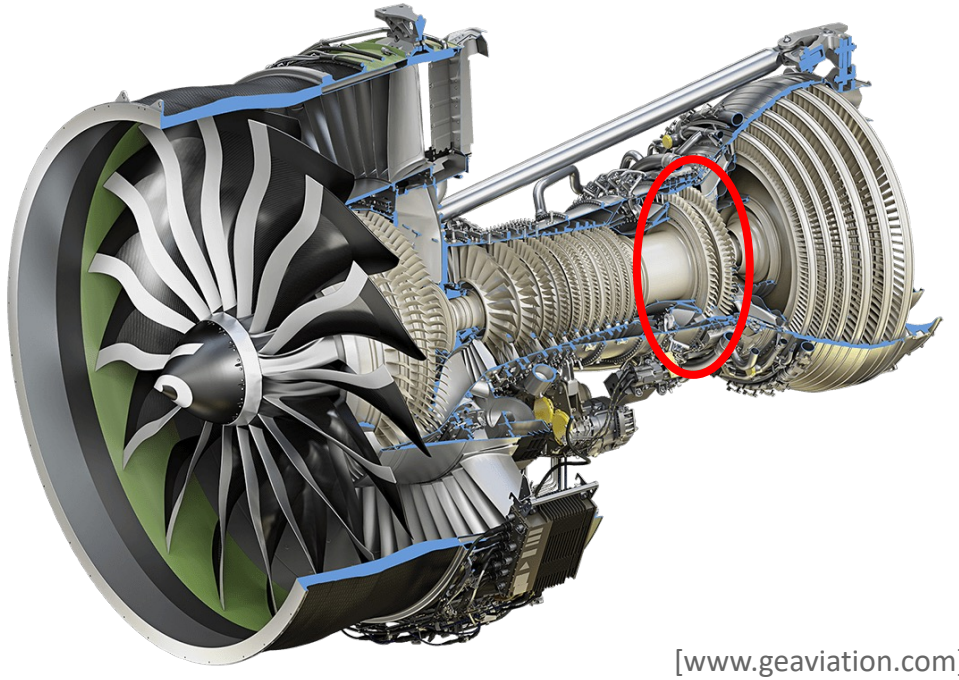

[www.geaviation.com]

LEAP engine (CFM)

# Ceramic Matrix Composites for aircraft engines

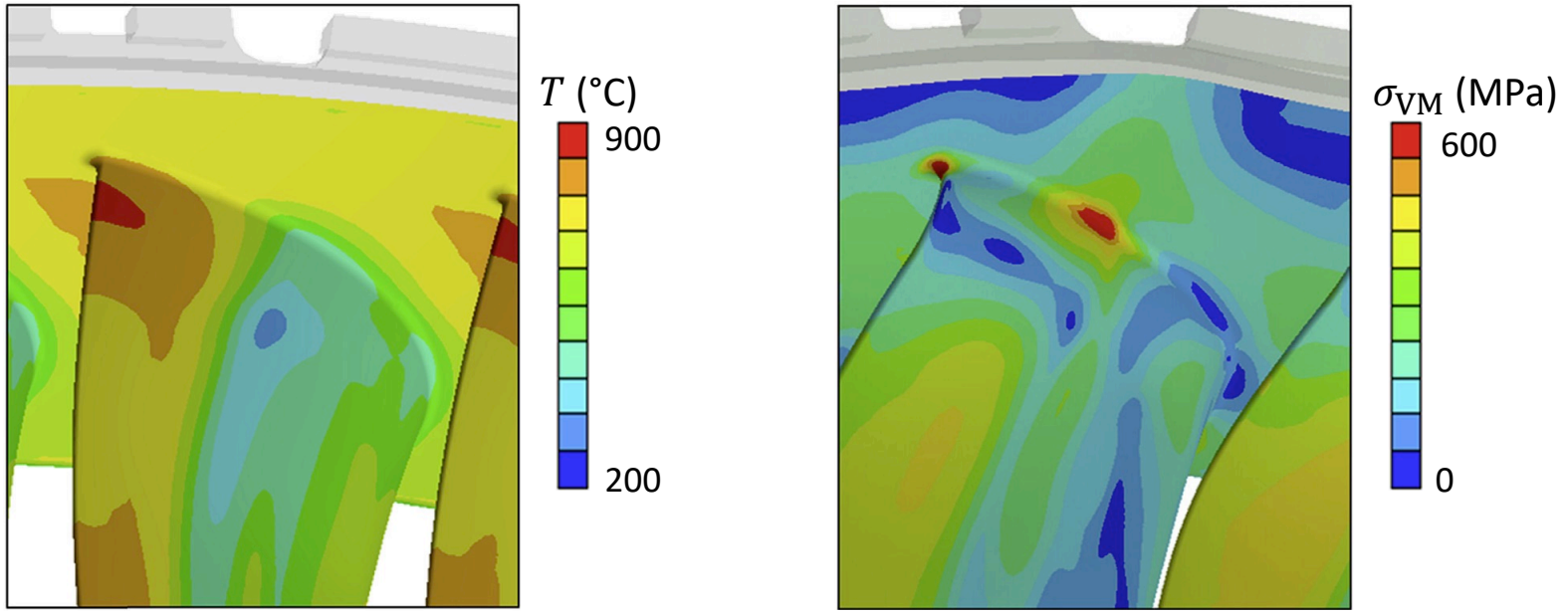


Temperature field

Von Mises eq. stress

[Chung, 2017]

Root of a superalloy fixed blade in operating condition

- Thermal loading + geometry → complex thermo-mechanical loading
- Influence of the meso-structure of CMCs?

# Influence of the meso-structure?

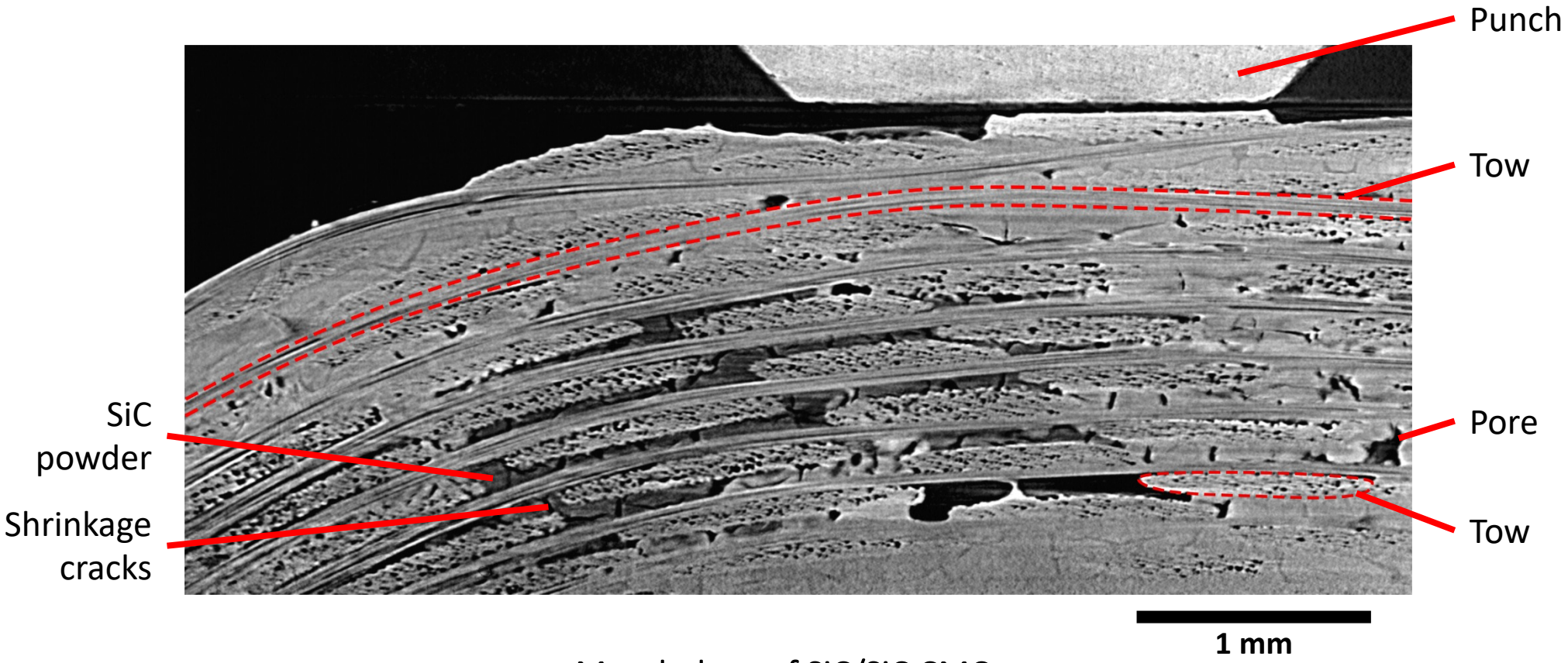


Morphology of SiC/SiC CMCs

# Meso-scale model

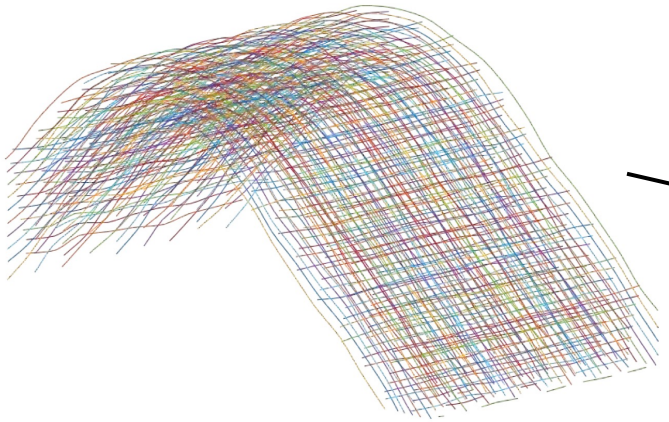

Simulated weaving

*from shaping of the woven pattern*

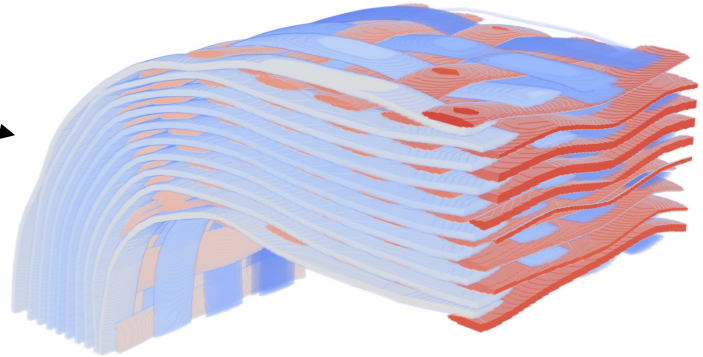

3D image of the weaving

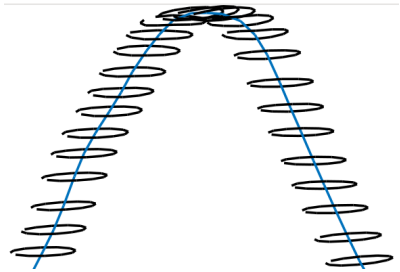

Textile descriptor

*neutral fibre and section*

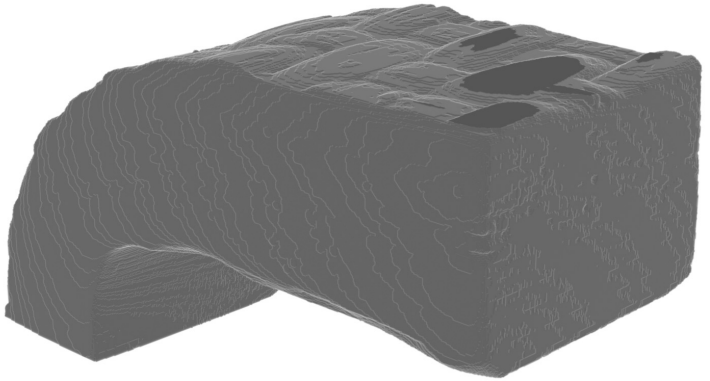

Binarised tomography

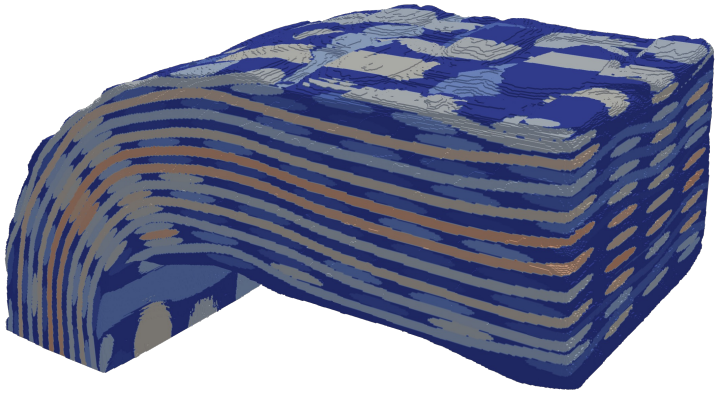

3D image of the mesostructure

# Meso-scale model

- Thermo-elastic phases
  - properties vary linearly with temperature
  - initial estimation from the literature
- Matrix
  - homogeneous, isotropic
  - $E, \nu, k$
- Tows
  - homogeneous, transverse isotropic
  - $E_{11}, E_{22}, \nu_{12}, \nu_{23}, G_{12}, G_{23}, k_{11} = k_{22} = k$
- Voids
  - isotropic with a very low Young Modulus

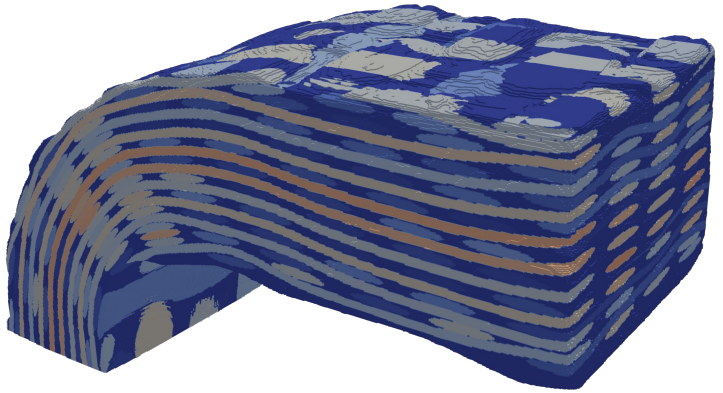

3D image of the mesostructure

# Local homogenisation strategy [Bénézech, PhD Th. 2019]

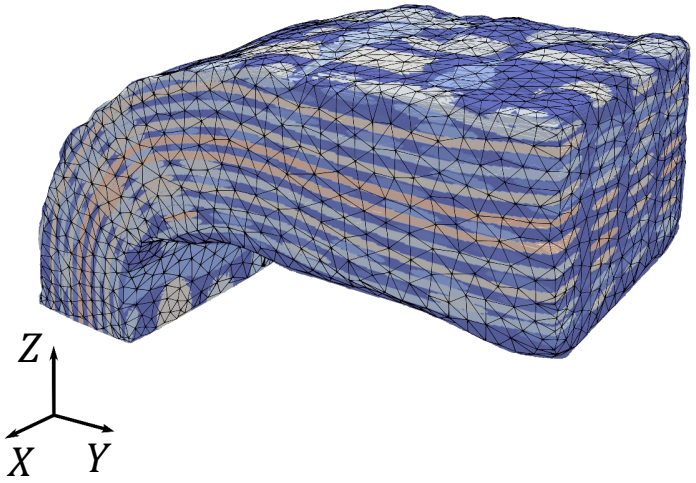


Macroscale mesh

*superimposed on the mesostructure*

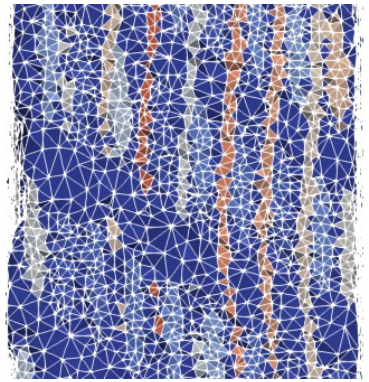

Conformal mesoscale mesh

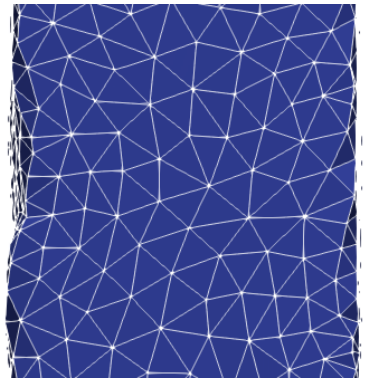

Macroscale mesh

$\mathbb{C}_{\text{eff.}} = \tau_i \mathbb{C}_i$

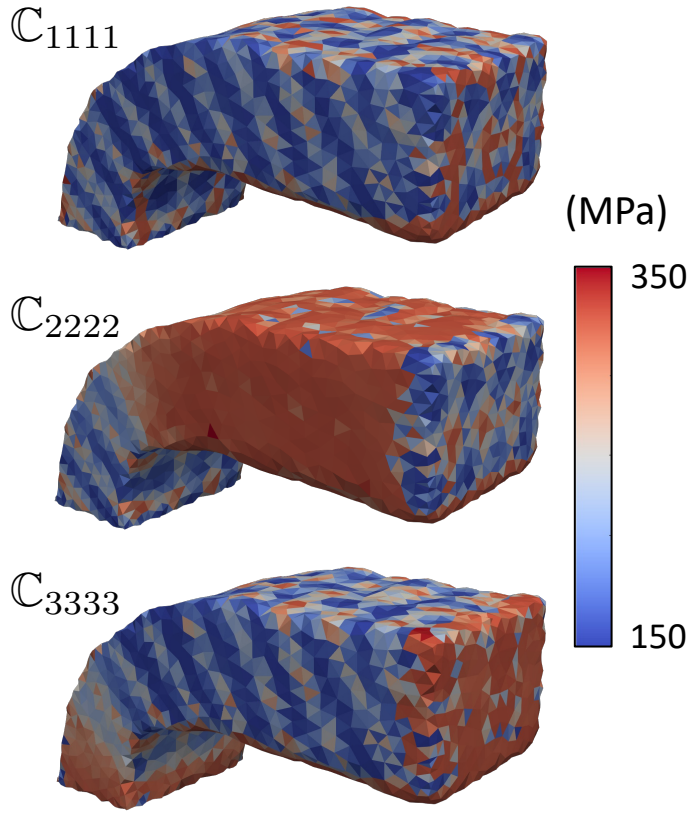


Fields of material properties

*from local homogenisation*

# Linking experiments and models

- Models
  - digital twin

  → fine description of the behaviour

## How to confront models to experiments?

→ Development of identification procedures

- experiment
- instrumentation (full-field measurement)
- identification itself

# In-situ thermomechanical experiment

- HT corner bending test
  - $T \simeq 500°\mathrm{C}$
  - $\nabla T \simeq 200°\mathrm{C.cm}^{-1}$
  - stepwise mechanical loading
  - full-field measurement

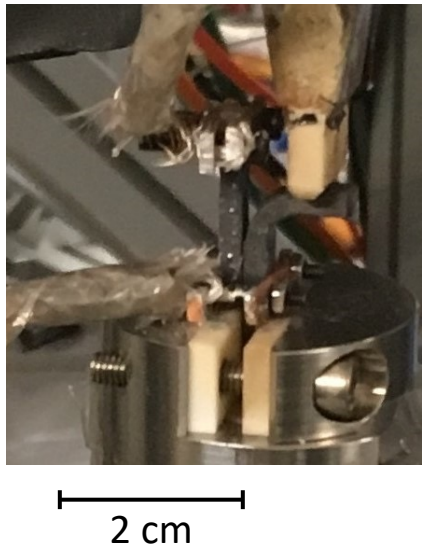


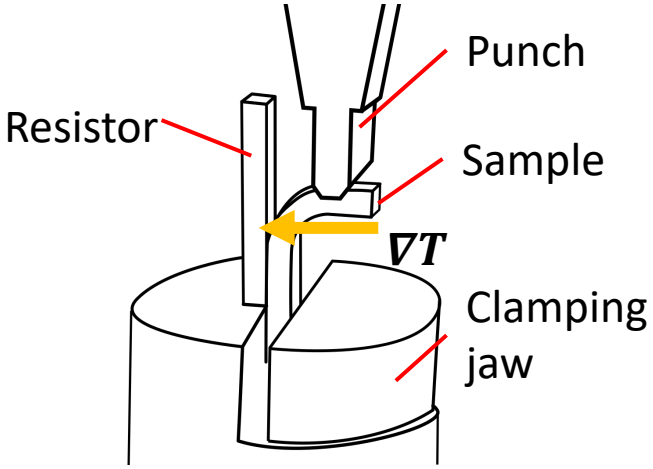


[Turpin, *J. Synchrotron Rad.*, 2022]

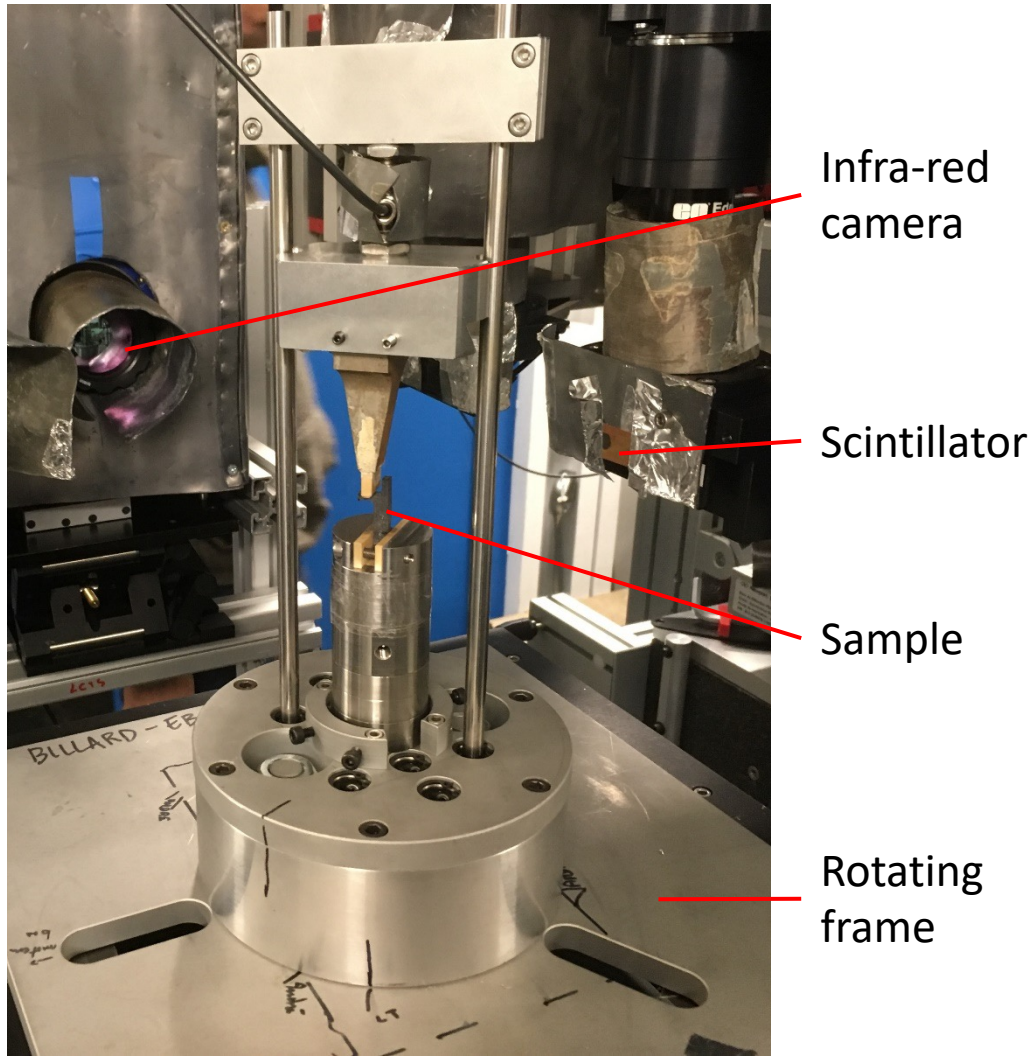

# Multi-modal full-field measurement

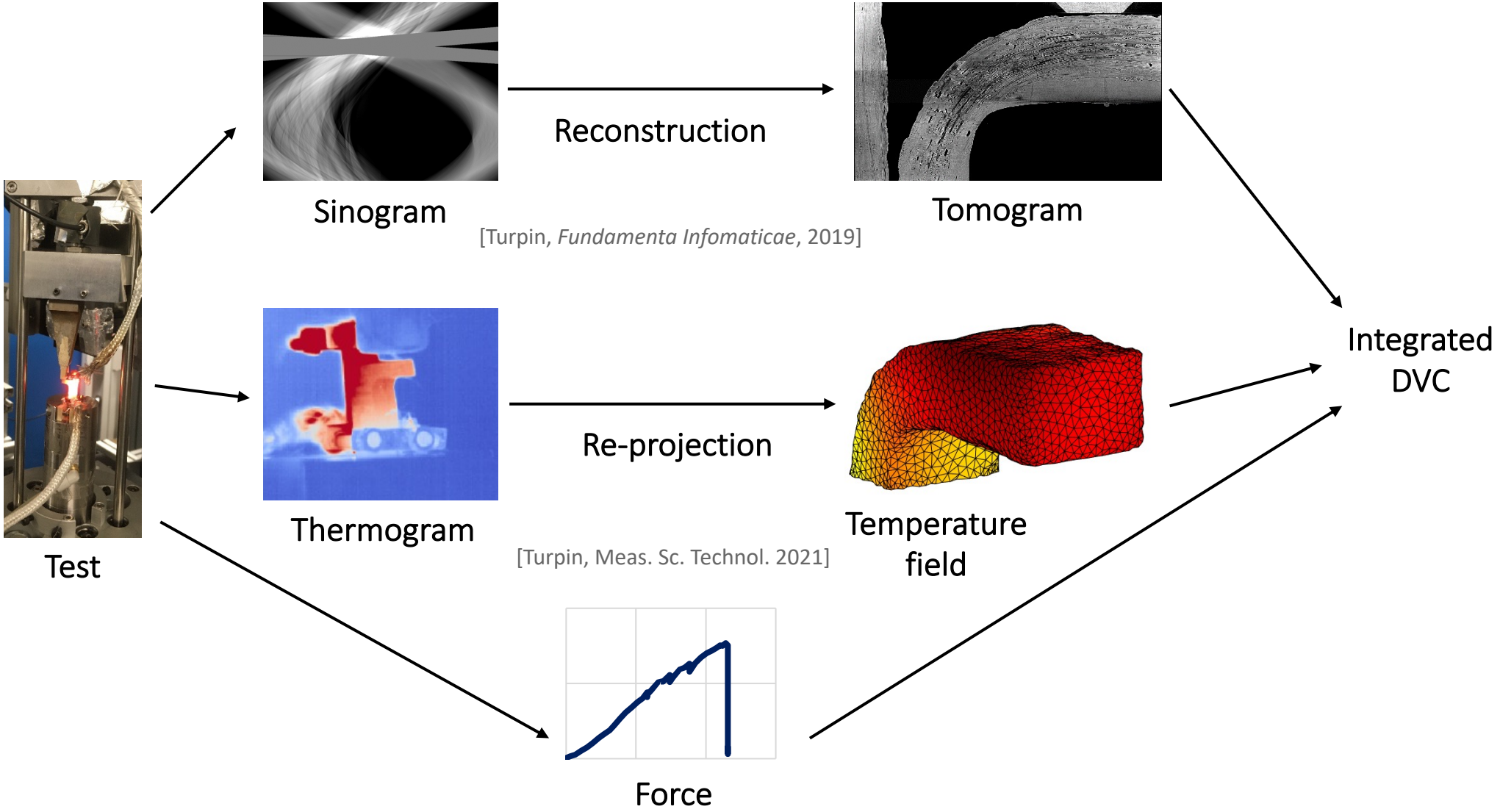

# Identification

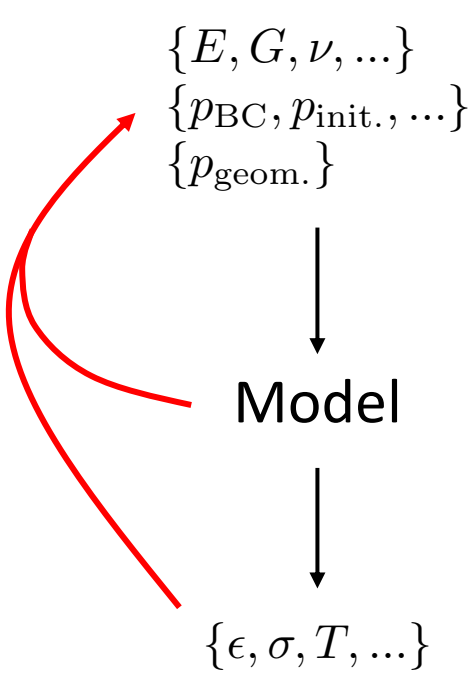


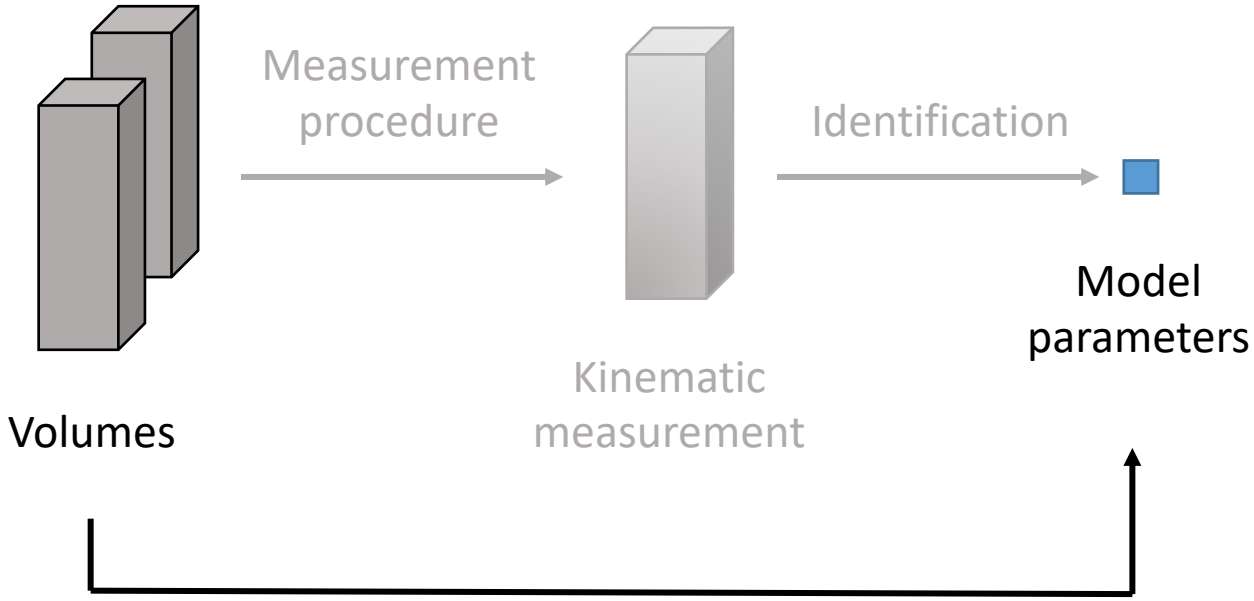


Integrated measurement process

In-situ test followed by tomography

# Digital Image/Volume Correlation (DIC/DVC)

- Global DIC [Hild & Roux, 2006]
  - displacement field $\boldsymbol{u}$ minimising of the residual, $\rho$

$$\rho(\boldsymbol{x}) = f(\boldsymbol{x}) - g(\boldsymbol{x} + \boldsymbol{u}(\boldsymbol{x}))$$

$$\boxed{\boldsymbol{u} = \arg\min \int_{\mathrm{ROI}} \rho^2 \mathrm{d}\boldsymbol{x}}$$

  - $\boldsymbol{u}$ is expressed on an FE basis, $\boldsymbol{\varphi}$

$$\boldsymbol{u}(\boldsymbol{x}) = a_i \varphi_i(\boldsymbol{x})$$

  - Gauss-Newton algorithm

$$[M]\{\mathrm{d}a\} = \{b\}$$

$$\begin{cases} [M] &= \displaystyle\int \varphi^{\mathrm{t}} \boldsymbol{\nabla} f^{\mathrm{t}} \boldsymbol{\nabla} f \varphi \, \mathrm{d}\boldsymbol{x} \\ \{b\} &= \displaystyle\int \varphi^{\mathrm{t}} \boldsymbol{\nabla} f^{\mathrm{t}} \rho \, \mathrm{d}\boldsymbol{x} \end{cases}$$

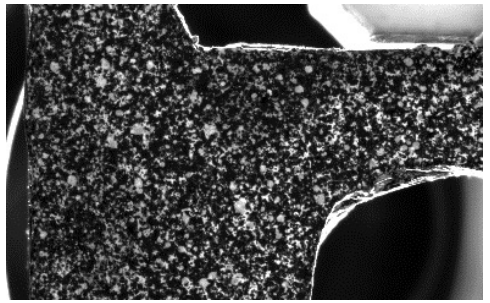

Reference image $f$

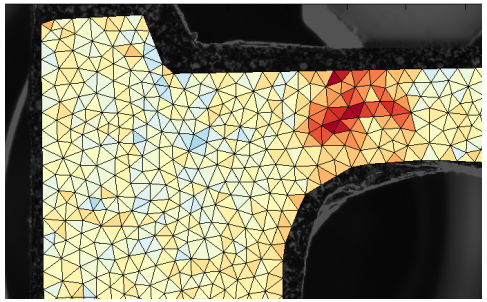

Deformed image $g$

# Integrated-DIC/DVC

- Global DIC

$$[M]\{\mathrm{d}a\} = \{b\} \qquad \begin{cases} [M] &= \int \varphi^{\mathrm{t}} \boldsymbol{\nabla} f^{\mathrm{t}} \boldsymbol{\nabla} f \varphi \, \mathrm{d}\boldsymbol{x} \\ \{b\} &= \int \varphi^{\mathrm{t}} \boldsymbol{\nabla} f^{\mathrm{t}} \rho \, \mathrm{d}\boldsymbol{x} \end{cases}$$

- Integrated-DIC [Leclerc, 2009]
  - $\boldsymbol{u}$ is expressed on any relevant basis, $\boldsymbol{\psi}$

$$[H]\{\mathrm{d}p\} = \{c\} \qquad \begin{cases} [H] &= \int \psi^{\mathrm{t}} \boldsymbol{\nabla} f^{\mathrm{t}} \boldsymbol{\nabla} f \psi \, \mathrm{d}\boldsymbol{x} \\ \{c\} &= \int \psi^{\mathrm{t}} \boldsymbol{\nabla} f^{\mathrm{t}} \rho \, \mathrm{d}\boldsymbol{x} \end{cases}$$

  - using sensitivity fields, $[S]$

$$S_i = \frac{\partial a}{\partial p_i} \qquad \begin{cases} [H] &= [S]^{\mathrm{t}}[M][S] \\ \{c\} &= [S]^{\mathrm{t}}\{b\} \end{cases}$$

# Integrated-DVC

- Weak thermomechanical coupling
  - measured temperature field is used as boundary conditions

- Coupling displacements and force

$$\begin{bmatrix} S_U \\ S_F \end{bmatrix}^{\mathrm{t}} \begin{bmatrix} \frac{M}{\sigma_f^2} & 0 \\ 0 & \frac{1}{\sigma_F^2} \end{bmatrix} \begin{bmatrix} S_U \\ S_F \end{bmatrix} \{\mathrm{d}\tilde{p}\} = \begin{bmatrix} S_U \\ S_F \end{bmatrix}^{\mathrm{t}} \begin{Bmatrix} \frac{b}{\sigma_f^2} \\ \frac{F_{\mathrm{mes}} - F_{\mathrm{EF}}}{\sigma_F^2} \end{Bmatrix}$$

  - identification of normalised parameters $\tilde{p}_i = \mathcal{N}(p_i)$

$$\tilde{E} = \frac{E}{E_{\mathrm{nom.}}} \qquad \tilde{\nu} = \nu \qquad \tilde{k} = \frac{\Delta T \ell}{u_{\mathrm{ref.}}} k$$

  - contributions weighted by their resp. uncertainty ($\sigma_f$ and $\sigma_F$)

# HT corner bending test

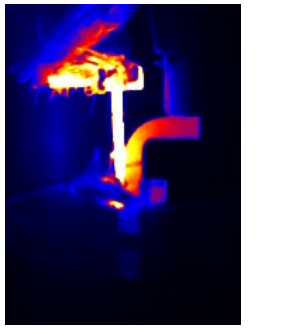


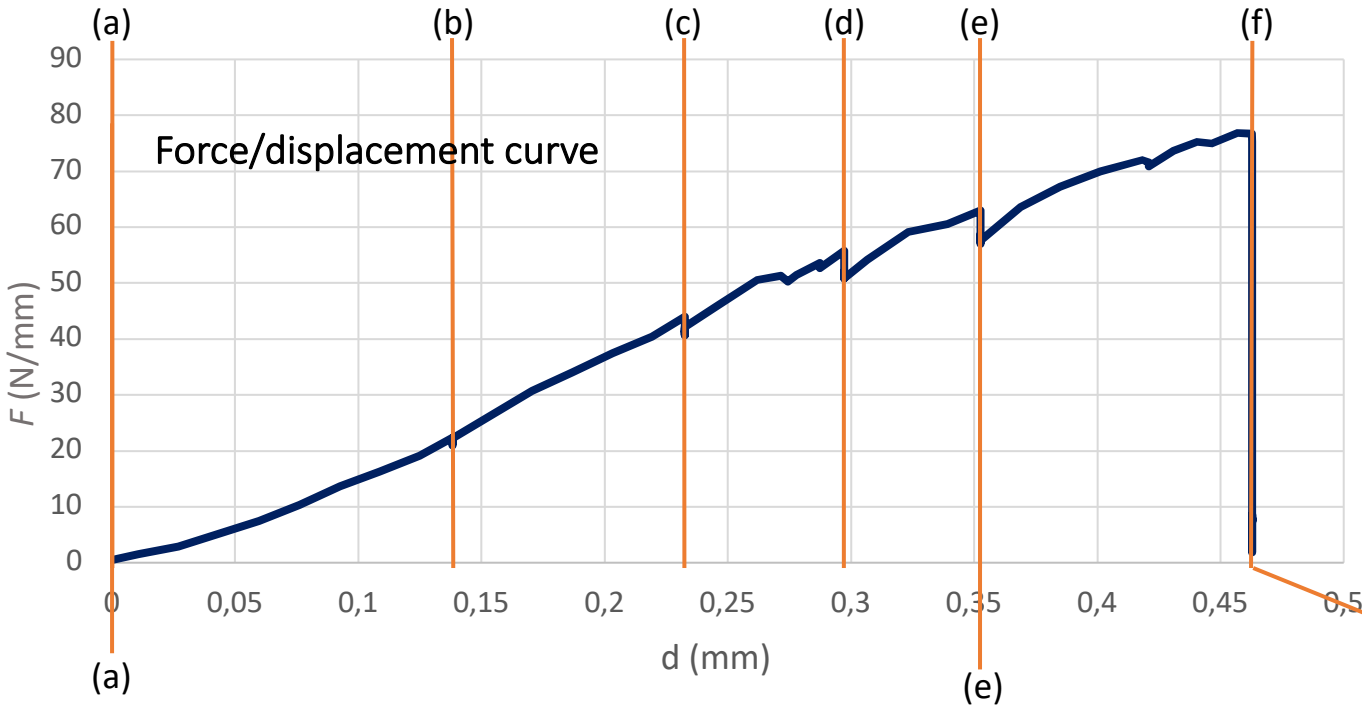


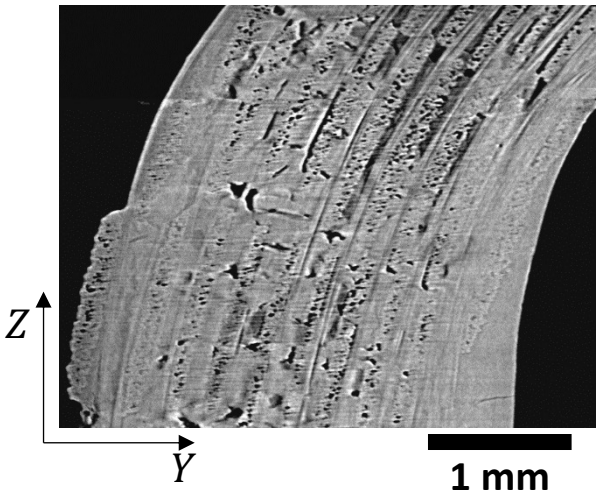


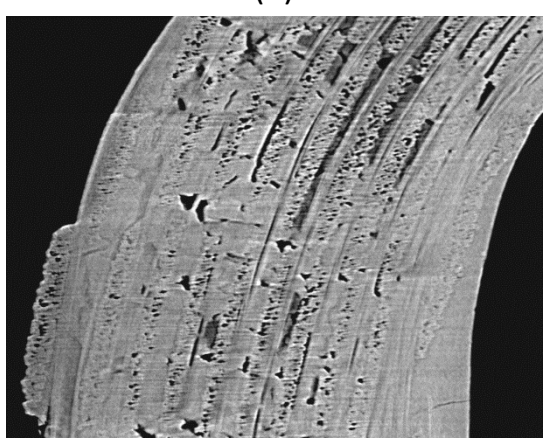


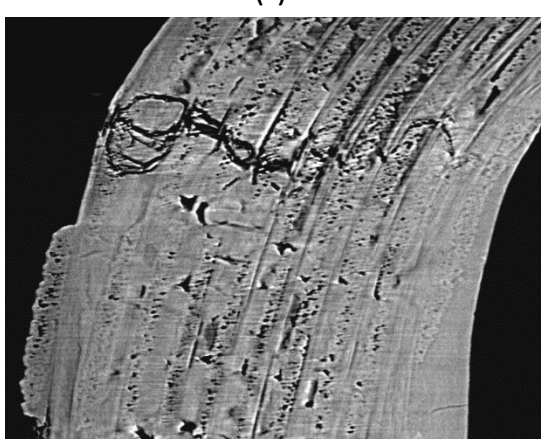

# HT corner bending test

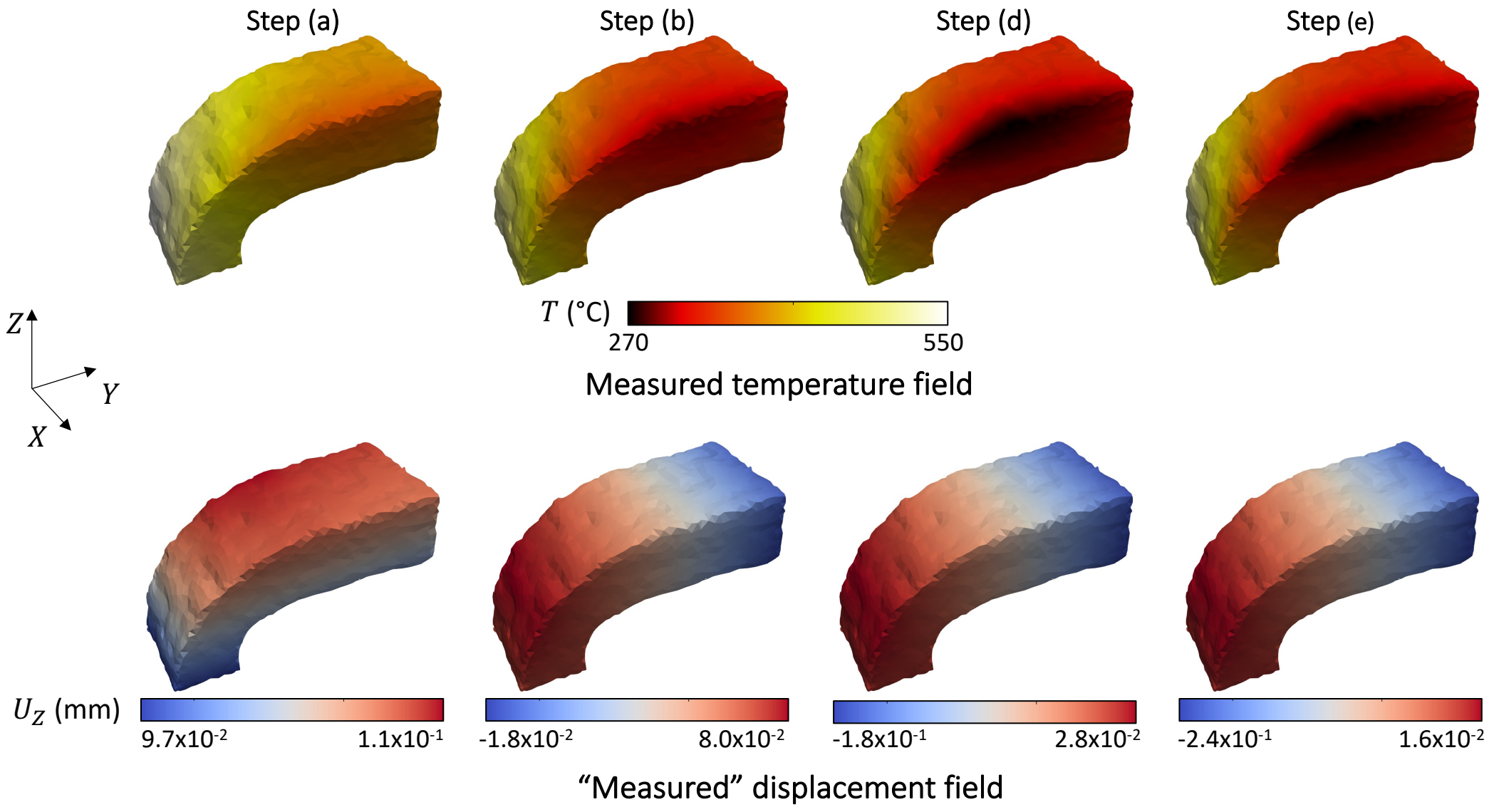

# HT corner bending test – Model validation

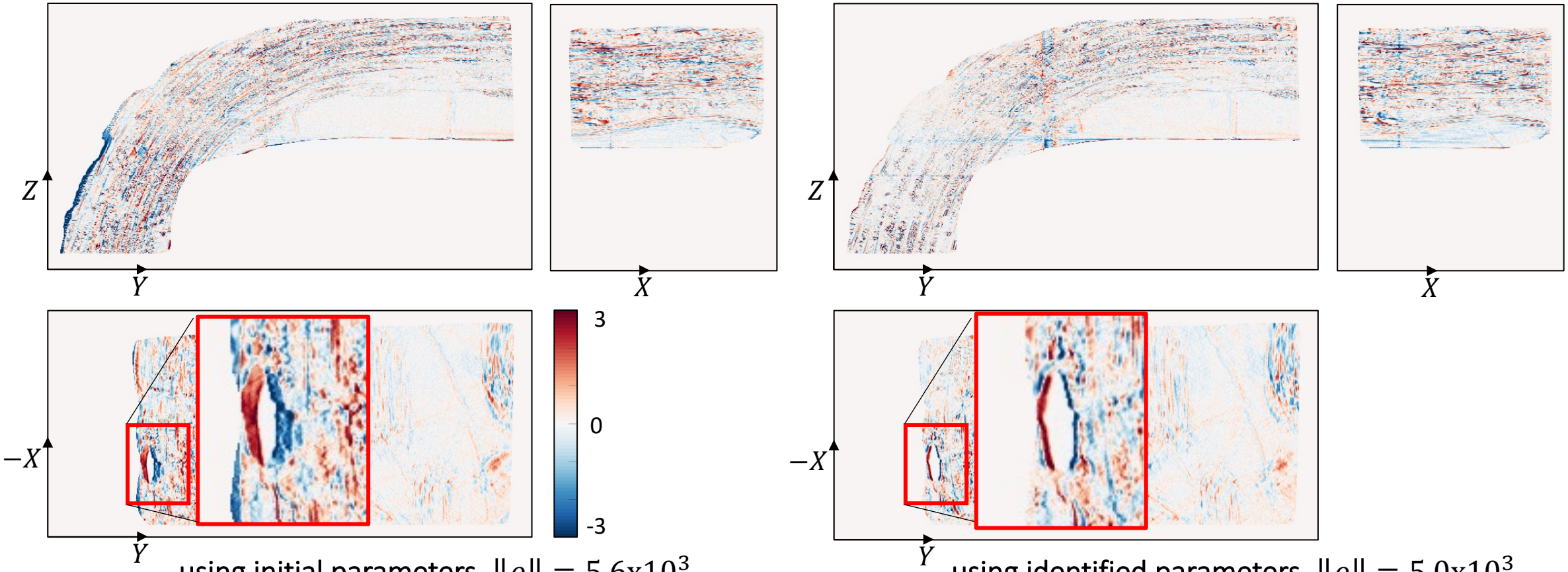


using initial parameters, $\|\rho\| = 5.6\text{x}10^3$

using identified parameters, $\|\rho\| = 5.0\text{x}10^3$

Residual field (loading step *b*)

$$\rho(\boldsymbol{x}) = f(\boldsymbol{x}) - g(\boldsymbol{x} + \boldsymbol{u}(p))$$

# HT corner bending test – Identification of material parameters

- Set of paramaters
  - 9 mesoscale constituant parameters
  - 2 temperatures

- Most of them are identified with a good uncertainty
  - $E_m(T_{\mathrm{amb}}) = 304 \pm 2\,\mathrm{GPa}$
  - $k(T_{\mathrm{amb}}) = 4.16.10^{-6} \pm 1.10^{-8}\ \mathrm{K}^{-1}$
  - $E_{22,t}(T_{\mathrm{amb}}) = 127 \pm 2\,\mathrm{GPa}$

- Some have greater uncertainty
  - $G_{12,t}(T_h) = 54 \pm 6\,\mathrm{GPa}$
  - $\nu_{23,t}(T_{\mathrm{amb}}) = 0.12 \pm 0.04$

# Conclusion and outlooks

- Enriched macro-scale model
  - good description of the material behaviour
- Identification problem
  - in-situ tomography + thermography
  - complex sample

  → closely link model and experiment

  → provide the best material parameter set
- Quantitative investigation about damage ?

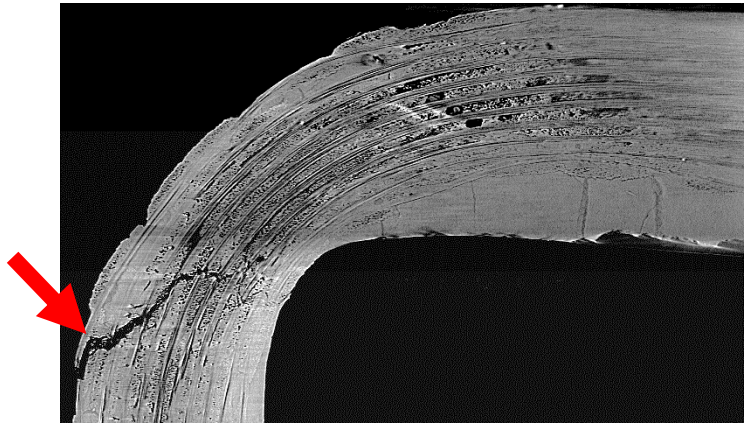

Tomogram, step (f)

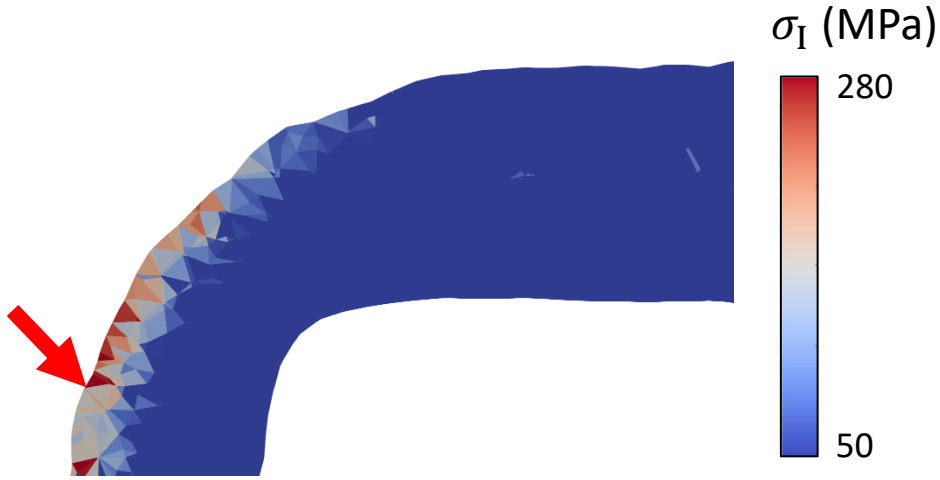


Max. Eigenstress

Thermography

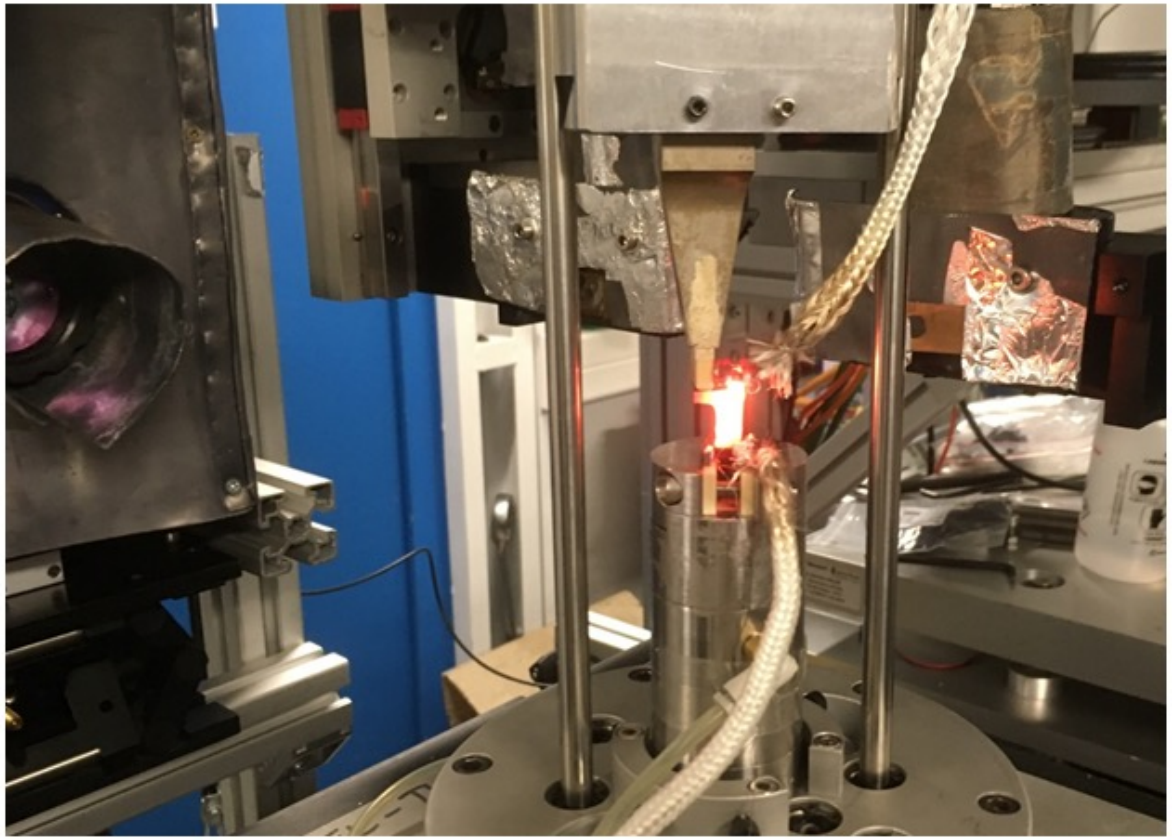

High mechanical and thermal loads for in-situ tomography of complex CMC parts (PSICHE, SOLEIL)

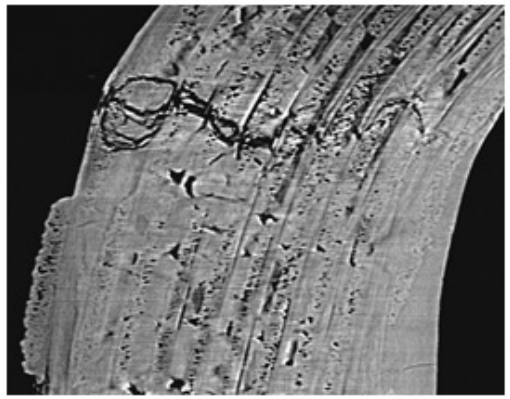

Tomography

# References


Bénézech, J., & Couégnat, G. (2019). Variational segmentation of textile composite preforms from X-ray computed tomography. *Composite Structures*, *230*, 111496. doi: 10.1016/j.compstruct.2019.111496

Turpin, L., Roux, S., Caty, O., & Denneulin, S. (2020). A phase field approach to limited-angle tomographic reconstruction. *Fundamenta Informaticae*, *172*(2), 203-219. doi: 10.3233/FI-2020-1901

Turpin, L., Roux, S., Caty, O., & Denneulin, S. (2020). Coupling tomographic and thermographic measurements for in-situ thermo-mechanical tests. *Measurement Science and Technology*, *32*(3), 035401. doi: 10.1088/1361-6501/abcc9f

Turpin, L., Roux, S., Caty, O., King, A., Denneulin, S., & Martin, É. (2022). In situ tomographic study of a 3D-woven SiC/SiC composite part subjected to severe thermo-mechanical loads. *Journal of Synchrotron Radiation*, *29*(2). doi: 10.1107/S1600577522000406

Turpin, L., Roux, S., Bénézech, J., Couégnat, G., King, A., Caty, O., Denneulin, S., & Martin, É. (under review) Quantitative thermomechanical characterisation of 3D-woven SiC/SiC composites from in-situ tomographic and thermographic imaging